Digital and Optical Reconstruction of Images from Suboptical Diffraction Patterns

T. H. Demetrakopoulos and R. Mittra

Digital and optical reconstruction techniques are applied to synthetic holograms that are recorded at suboptical frequencies. The first section of the paper considers digital reconstruction that entails the application of the inverse diffraction transform to the diffraction pattern of an object illuminated with a suboptical source. Different cross sections of the object are displayed on a CRT in a sequential fashion. Image enhancement techniques are also employed in the process of digital reconstruction. The second section outlines a method for partially alleviating the longitudinal distortion that is inherent in optical reconstruction from synthetic holograms because of the difference between the recording and reconstructing wavelengths. The paper considers both the diffuse and nondiffuse illumination schemes and discusses the relative advantages and disadvantages of digital and optical reconstruction schemes.

I. Introduction

Optical reconstruction applied to holograms that have been recorded at suboptical frequencies (acoustic or microwave) produces a longitudinally distorted image unless the original hologram has been reduced by the factor $1/\mu$, where $\mu = \lambda_2/\lambda_1$, and λ_1, λ_2 are the recording and reconstruction wavelengths, respectively.[1] The scaling factor $1/\mu$ is in most cases very large and difficult to achieve. However, even if perfect scaling takes place, the final image will be very small, thus, of questionable value.

In this paper we discuss two techniques for image reconstruction from suboptical holograms, both of which are designed to alleviate the problem mentioned above. We first consider some aspects of digital reconstruction and then describe a technique for partially alleviating the problem of longitudinal distortion in optical reconstruction schemes.[2] A comparison of the relative advantages and disadvantages of the digital and optical reconstruction schemes is also included.

II. Digital Reconstruction

In suboptical holography an object is typically illuminated using acoustic or microwave sources, and its diffraction pattern is recorded over an aperture using a suitable probing system. Assume that a sampled amplitude and phase pattern at the recording plane are available. For digital reconstruction this information is entered into the computer and processed using the inverse diffraction transform.[3] Then the object field can be approximately reproduced at various distances from the recording aperture. Although a similar approach has been previously applied to two-dimensional objects, in this paper we extend this procedure to objects with depth information.[4,5] In addition we consider the effect of both the diffuse and nondiffuse illumination and illustrate the use of nonlinear digital processing of the reconstructed images. Digital processing allows one to enhance the desired image and to suppress the undesired out-of-focus contributions to the image field at a given cross section.

Let $f_1(r_1)$ be the complex wavefront of the diffraction pattern in the plane $z = z_1$ as shown in Fig. 1. For purposes of this investigation we simulate the forward diffraction pattern in a computer by evaluating the diffracted field due to an object illuminated by a given source. It is useful to note that for digital reconstruction the recording process can deviate from conventional holography, since it is not necessary to introduce a reference wave during the recording process. The linear detectors used to sample the diffraction pattern can detect both the amplitude and phase of the scattered field, in contrast to the photographic film, which can record only the intensity. Thus, it is necessary to use the arrangement shown in Fig. 2 only when one plans to use optical methods for reconstruction. For the digital approach the reference wave may be omitted from the setup in Fig. 2.

The forward diffracted field of the object may be evaluated by using the Rayleigh-Sommerfeld diffraction formulas.[6] For a plane wave illuminating a

When this work was done both authors were with the University of Illinois, Urbana, Illinois 61801; T. H. Demetrakopoulos is now with the Chrysler Corporation, Sterling Heights, Michigan 48077.

Received 28 June 1973.

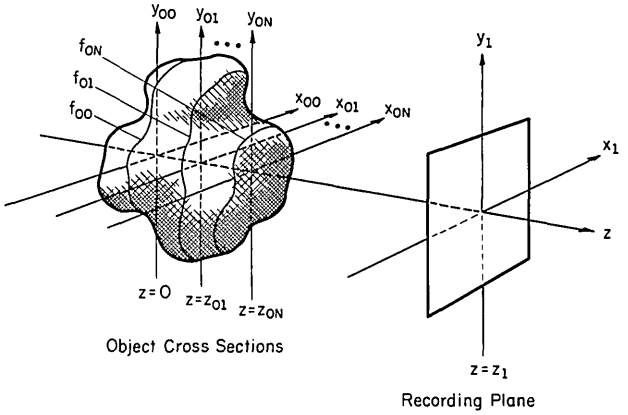

Fig. 1. Geometrical arrangement for recording of diffraction pattern.

transparency located at $z = z_o$, the field distribution at the plane $z = z_1$ is given by

$$f_1(x_1, y_1, z_1) \approx \iint_{S_o} f_o(x_o, y_o, z_o) g(x_1 - x_o, y_1 - y_o, z_1 - z_o) dS_o, \quad (1)$$

where $g(x_1 - x_o, y_1 - y_o, z_1 - z_o)$ is the propagator function given by

$$g(x_1 - x_o, y_1 - y_o, z_1 - z_o) \approx \frac{\exp(ik|r_1 - r_o|)}{i\lambda(z_1 - z_o)}, \quad (2)$$

where $|r_1 - r_o| = [(x_1 - x_o)^2 + (y_1 - y_o)^2 + (z_1 - z_o)^2]^{1/2}$ and (x_o, y_o, z_o), (x_1, y_1, z_1) are the coordinates of the object and recording planes, respectively. The integral in Eq. (1) is evaluated over the aperture S_0 in the plane $z = z_o$.

A three-dimensional object can be considered to be made up of an infinite number of planar cross sections. In practice we model three-dimensional objects that consist of a finite number of planar cross sections, as shown in Fig. 2. The cross sections are taken to be perpendicular to the z axis, at distances $n\Delta z$ from the plane $z = 0$, where $n = 0, 1, 2, \ldots, N$. Then the object $f_o(x_o, y_o, z_o)$ can be approximately described by[2]

$$f_o(x_o, y_o, z_o) = \sum_{n=1}^{N} \delta(z_o - z_{on}) f_{on}(x_{on}, y_{on}), \quad (3)$$

where $f_{on}(x_{on}, y_{on})$ is the planar distribution of the object on the nth plane for a total of N such planes. The planar distribution functions are space-limited functions. Moreover, for computational purposes each object plane is assumed to consist of a finite number of points. Under these conditions one may write

$$f_o(x_o, y_o, z_o) = \sum_{n=0}^{N} \delta(z_o - z_{on}) \sum_{i=1}^{I} \sum_{j=1}^{J} f_{on}(x_o, y_o) \delta(x_o - i\Delta x) \delta(y_o - j\Delta y) = \sum_{n=0}^{N} \delta(z_o - z_{on}) \sum_{i=1}^{I} \sum_{j=1}^{J} f_{on}(i\Delta x, j\Delta y), \quad (4)$$

where $I \times J$ is the number of scattering centers in each planar distribution, and Δx, Δy are the spatial sampling periods in the x and y directions, respectively. We assume that the points are uniformly distributed on each object plane, and for simplicity Δx equals Δy.

Equation (4) describes an object whose points all radiate in phase. However, this may not always represent the physical case in which the points may radiate independently of each other, which is the case of diffuse illumination, i.e., the relative phase of the wave scattered by each point is a random variable.[6] In this case, each point in Eq. (4) is multiplied by the factor $\exp(j2\pi R_{ij})$. Thus we have

$$f_o(x_o, y_o, z_o) = \sum_{n=0}^{N} \delta(z_o - z_{on}) \sum_{i=1}^{I} \sum_{j=1}^{J} f_{on}(i\Delta x, j\Delta y) \exp(i2\pi R_{ij}), \quad (5)$$

where R_{ij} is a uniformly distributed random variable with $0 \leq R_{ij} \leq 1$, and $2\pi R_{ij}$ is the relative phase of the wave scattered from the point scatterer located at $x_o = i\Delta x$, $y_o = j\Delta y$. Both nondiffuse and diffuse illuminating objects represented by Eqs. (4) and (5) have been considered. At the end of this section we will show that the image of a diffusely illuminated object is covered with the well-known grainlike noise or speckle pattern.

Substituting $f_o(x_o, y_o, z_o)$ from Eq. (3) into Eq. (1), we may obtain the diffraction pattern

$$f_1(x_1, y_1, z_1) \approx \sum_{n=0}^{N} \frac{1}{i\lambda(z_1 - z_{on})} \iint_{S_{on}} f_{on}(x_{on}, y_{on}) \exp(ik|r_1 - r_{on}|) dS. \quad (6)$$

The integration in Eq. (6) extends over the various cross-sectional planes S_{on} of the object from $z = 0$ to $z = z_{on}$. It should be pointed out that the effect of blockage, if any, is not reflected in Eq. (6). However, this effect can be accounted for in the above equation with some modification.

The integral in Eq. (6) is the convolution of the

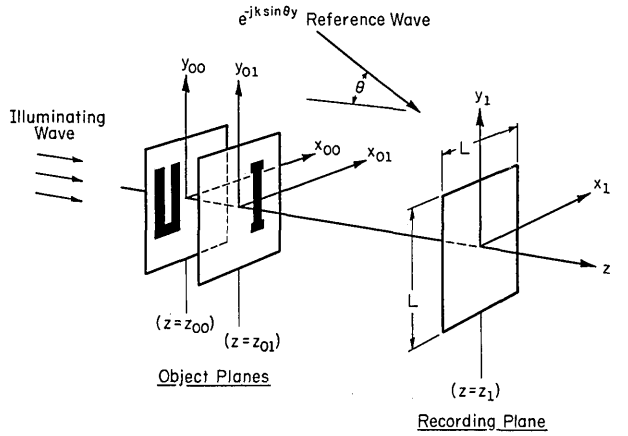

Fig. 2. Recording of hologram.

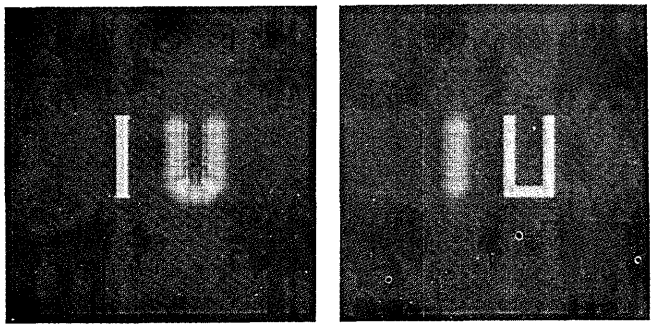

(a) Letter U out of focus. (b) Letter I out of focus.

Fig. 3. Digitally reconstructed cross sections of object shown in Fig. 2. Nondiffuse illumination was used.

function $f_{on}(x_{on},y_{on})$ with the propagator function $g(x_1 - x_{on}, y_1 - y_{on})$, i.e.,

$$f_1 = f_o * g, \tag{7}$$

where * implies convolution and g is defined by Eq. (2). Applying the well-known convolution theorem, we find

$$f_1 = \sum_{n=0}^{N} F^{-1}[F_{on}G_{on}], \tag{8}$$

where F_{on}, G_{on} are the Fourier transforms of f_{on}, g_{on}, respectively, and N is the number of cross sections. Equation (8) is evaluated through the use of the fast Fourier transform (FFT) algorithm.[8,9] We also note that G_{on}, the Fourier transform of g_{on}, may be evaluated analytically, and the Fourier transform of f_{on} must be computed by the FFT routine.

In order for the discrete sampling array to represent the diffraction $f_1(r_1)$, the spatial rate of sampling must satisfy the sampling theorem.[10] The numerical evaluation of Eq. (8) was performed on the IBM model 360/75 computer, and the two-dimensional 128 × 256 sampling array was stored on a magnetic tape. Digital processing of these data yields the reconstructed object field, as shown in the following paragraph.

A method for an exact inversion of the diffracted field to recover the object field has been given by Mittra and Ransom.[2] Because the exact formulas are computationally involved, suitable approximations must be employed to make the method numerically viable. The use of the Fresnel approximation leads to the equation

$$f_{on}(r_{on}) \approx \int\int_{S_1} f_1(r_1)\tilde{g}(r_{on}, r_1)dS_1, \tag{9}$$

where $\tilde{g}$ is the approximate inverse of the propagator g and is given by

$$\tilde{g}(r_{on}, r_1) = \frac{\exp(-ik|r_1 - r_{on}|)}{-i\lambda|r_1 - r_{on}|}. \tag{10}$$

In Eqs. (9) and (10) the subscript n refers to the nth planar cross section of the object. Thus, $r_{on} = (x_{on},y_{on},z_{on})$ and $|r_1 - r_{on}| = [(x_1 - x_{on})^2 + (y_1 - y_{on})^2 + (z_1 - z_{on})^2]^{1/2}$. The approximations used in obtaining Eq. (9) have been discussed by Lalor.[11] After substitution of Eq. (10) in Eq. (9) we obtain

$$f_{on}(x_{on}, y_{on}, z_{on}) \approx \int\int f_1(r_1) \frac{\exp(-ik|r - r_{on}|)}{-i\lambda|z_o - z_{on}|} dS_1. \tag{11}$$

The convolution integral in Eq. (11) is again evaluated using the fast Fourier transform algorithm. For the nth cross section of $f_o(r_o)$ we have

$$f_{on}(r_{on}) \approx F^{-1}\left\{F[f_1(r_1)]F\left[\frac{\exp(-ik|r_1 - r_{on}|)}{i\lambda(z_1 - z_{on})}\right]\right\}. \tag{12}$$

Equation (12) indicates that for any value of $z_1 - z_{on}$, we can propagate backward to any desired distance from the recording plane. It is not necessary to know the distance $z_1 - z_{on}$ *a priori* to locate the object. One merely propagates backward until there is an indication of the location of the object as evidenced by the appearance of a reconstructed image on the CRT display that is used to view the object. This process is continued and the distance z_1 (= z_{on}) is progressively increased to reconstruct the entire object.

Figures 3(a) and 3(b) show cross sections of the reconstructed image for the object shown in Fig. 2. The object was considered to be nondiffusely illuminated, as described by Eq. (4). Figure 3(a) shows that the letter U is out of focus, while in Fig. 3(b) the letter I is out of focus. Figures 4(a) and 4(b) show cross sections of the reconstructed image for the object shown in Fig. 2; however, the object was simulated to have diffuse illumination as described by Eq. (5). As expected, the speckle pattern appears in this case. When the digital reconstruction method is used, the entire image of the object is not

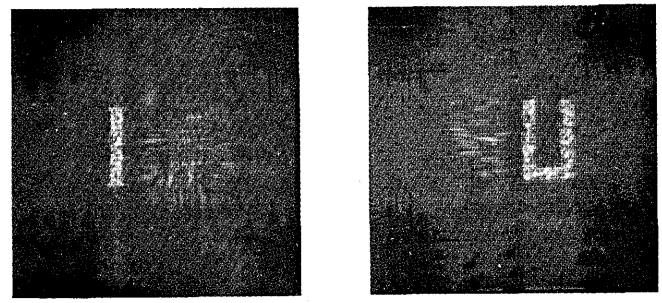

(a) Letter U out of focus. (b) Letter I out of focus.

Fig. 4. Digitally reconstructed cross sections of object shown in Fig. 2. Diffuse illumination was used.

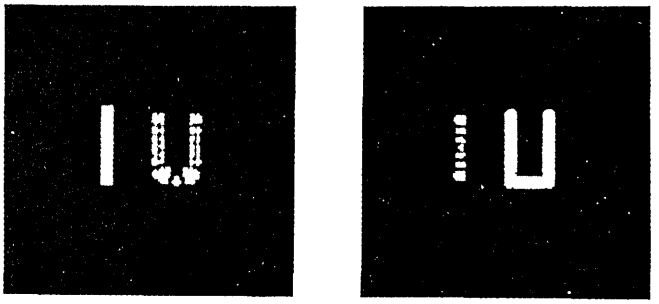

(a) (b)

Fig. 5. Two-level quantization in the intensity of Fig. 3 (a), (b). Intensity of points $I = 250$ if $I \geq 150$. (Scale $0 \rightarrow 255$.)

displayed simultaneously; rather, various cross sections of the object are shown sequentially on the CRT display. Moreover, for 3-D objects, undesired, out-of-focus information in the image plane is present. However, image enhancement techniques can be applied to the reconstructed images before their final display on the CRT, and the contribution of the out-of-focus images in a given cross section can be reduced. The reduction can be accomplished by thresholding. To illustrate this procedure, thresholding was applied to the images shown in Figs. 3 and 4, and the resulting images are shown in Figs. 5 and 6, respectively. The suppression of out-of-focus information is evident in the last two figures. Digital processing also allows the flexibility of other types of linear and nonlinear processing of the image.

III. Optical Reconstruction and Alleviation of Longitudinal Distortion

In many situations the entire three-dimensional image can be visualized through optical reconstruction. However, optical reconstruction from suboptical synthetic holograms produces a longitudinally distorted image; the reasons were discussed in Sec. I. A method of partially alleviating the problem of longitudinal distortion occurring in reconstructed images of 3-D objects will now be described. After the cross sections of the image were digitally reconstructed, as indicated in Sec. II, image-enhancement techniques are applied to reduce the out-of-focus contributions. Next, the reconstructed object is longitudinally reduced, and a synthetic hologram of this predistorted version of the object is constructed using one of several available methods[12,13] for computer generation of holograms. Subsequently, when an optical wave is used for reconstruction, longitudinal magnification occurs because of the difference between the recording and reconstructing wavelengths. The longitudinal reduction, which was introduced during the recording of the synthetic hologram, partially compensates for the longitudinal magnification introduced in the reconstruction process. However, the depth of focus limits the method from completely eliminating the longitudinal distortion.

In order to computer synthesize a hologram for a given object, the forward diffraction pattern of the object must be evaluated. The geometric arrangement for computing the forward diffraction pattern is shown in Fig. 2. The diffraction pattern f_1 is evaluated as shown in Sec. II. Next, a plane reference wave of the form is introduced

$$U_r = S \exp(-ik \sin \theta y_1), \tag{13}$$

where S is a constant and θ is the angle that the propagation vector k makes with the normal to the hologram. The intensity on the hologram at $z = z_1$ then is

$$I(x_1, y_1, z_1) = |f_1(x_1, y_1, z_1) + S \exp(-ik \sin \theta y_1 \tag{14}$$

In synthetic holography the recording of the intensity is carried out by digital sampling of I over the area of the hologram. Again, in order for the discrete sampling array to accurately represent the intensity I, the spatial sampling rate must satisfy the sampling theorem.

The two-dimensional sampling array of the intensity was plotted on a high resolution, high contrast cathode ray tube. Because of the limitations of the computer memory, a small array of 128 × 128 points was used. Then a photographic transparency was made of the CRT display. The photographic transparency, which was optically reduced to an area of 0.635 × 0.635 mm^2, was used in the subsequent optical reconstruction.

Figure 7 shows a diagram of the experimental setup used for the optical reconstruction. The holographic transparency is illuminated by a collimated beam originating from a He–Ne laser. The holo-

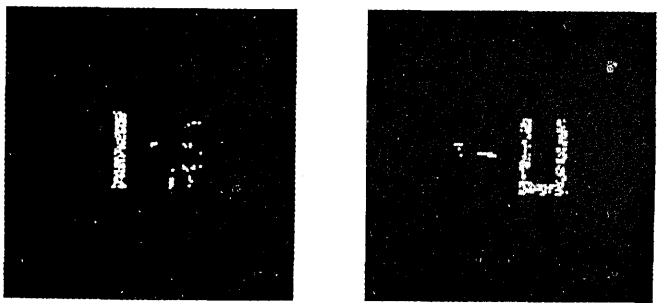

(a) (b)

Fig. 6. Two-level quantization in the intensity of Fig. 4, (a) (b). Intensity of points $I = 250$ if $I \geq 100$. (Scale $0 \rightarrow 255$.)

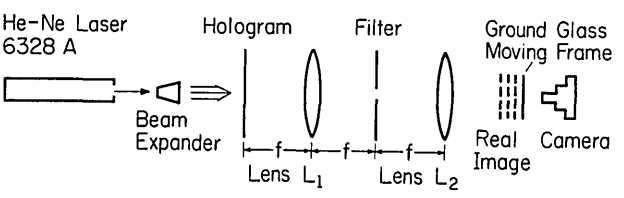

Fig. 7. Diagram of experimental setup for optical reconstruction.

(a) (b)

Fig. 8. Optically reconstructed images. In (a) the letter U is out of focus, in (b) the letter I is out of focus.

gram described in the previous section consists of a mesh of variable intensity points and can be represented as a finite, two-dimensional grating in the form

$$h_s(x,y) = \sum_{n=-(N/2)}^{(N/2)-1} \sum_{m=-(M/2)}^{(M/2)-1} h(nd,md)\delta(x - nd)\delta(y - md), \tag{15}$$

where $d = \Delta x = \Delta y$ is the sampling period. When such a hologram is placed in the front focal plane of the lens L_1, the field distribution on the back focal plane of L_1 is its Fourier transform $H_s(f_x,f_y)$, which is given by

$$H_s(f_x,f_y) = \sum_{n=-(N/2)}^{(N/2)-1} \sum_{m=-(M/2)}^{(M/2)-1} H[f_x - (n/d), f_y - (m/d)]. \tag{16}$$

Equation (16) indicates that a multiplicity of diffracted orders appears on the back focal plane because of the discrete, sampled nature of the hologram. When a spatial filter is inserted in the second focal plane of lens L_1, as shown in Fig. 7, all but the desired first-order wave is removed from the back focal plane. The second lens performs the Fourier transform of the distribution that is present in its front focal plane, and the real image is formed further back from the back focal plane of lens L_2, as shown in Fig. 7, all but the desired first-order wave is removed from the back focal plane. The second lens performs the Fourier transform of the distribution that is present in its front focal plane, and the real image is formed further back from the back focal plane of lens L_2.

The setup shown in Fig. 7 enables one to photograph any cross section of the real image by projecting it on a diffusing screen and properly focusing the camera. Figures 8(a) and 8(b) illustrate some image cross sections obtained in this manner for the object shown in Fig. 2. Figure 8(a) shows part of the image; the letter U is out of focus, while in Fig. 8(b) the letter I is out of focus. Recall that when the distance between the letters I and U in the recording process is reduced, the distance in the final image between the letters I and U is also reduced, thus compensating for the longitudinal distortion. The large depth of focus in synthetic holographic imaging can be explained as follows. The depth of focus in holographic imaging, which is analogous to the depth of focus in conventional imaging,[13] is given by

$$\Delta z' = \pm 2(z_i^2/D_1)\lambda_2, \tag{17}$$

where z_i is the image-to-hologram distance, D_1 is the aperture of the hologram, and λ_2 is the viewing wavelength. Equation (17) shows that the high λ/D_1 ratio occurring in synthetic holography, as compared with the low wavelength-to-aperture ratio in conventional imaging, is responsible for a large depth of focus in synthetic holographic imaging. This large depth of focus limits the technique from reducing the longitudinal magnification, and only partial compensation of the distortion by the method outlined above is possible.

IV. Discussion

In this investigation our aim has been to reconstruct images of three-dimensional objects from diffraction patterns recorded at suboptical frequencies. Two methods for such a reconstruction were applied: optical and digital. For the optical reconstruction method, a technique for reducing the longitudinal distortion of the image in synthetic holograms is introduced. This technique allows one to partially, but not completely, reduce the longitudinal distortions due to the large depth of focus present. However, it is an improvement over the case where the technique is not applied.

Both the optical and digital reconstruction methods have some advantages and disadvantages. The major advantage of the optical method is that it gives 3-D images, but its major disadvantage is that it yields a very small image. Larger apertures (more sampling points), along with improvements on the resolution of the displaying system for the recording of holograms, can be employed to improve the optical reconstruction technique. The digital reconstruction method is simpler, eliminates photographic processing, and gives larger images than the optical reconstruction method. However, only a two-dimensional cross section of the image can be displayed at any one time. Furthermore, out-of-focus contributions, which are present at each planar cross section of the reconstructed object, degrade the image quality. Image enhancement may be employed to partially circumvent this problem.

With advances in computer technology, digital reconstruction techniques will play an increasingly larger role in imaging and displaying. If a real-time imaging capability system is achieved, the digital reconstruction will become the dominant method of reconstructing images from suboptical diffraction patterns.

This work was supported in part by the Joint Services Electronics Program (U.S. Army, U.S. Navy, and U.S. Air Force) under Contract DAAB07-72-C-0259, and in part by the Army Research Office-Durham under Grant DA-ARO-D-31-124-G77.

References

1. R. Meier, J. Opt. Soc. Am. **55**, 987 (1965).
2. T. H. Demetrakopoulos and R. Mittra, Opt. Soc. Am. 1973 Spring Meeting Program, p. 15 (1973).
3. R. Mittra and P. L. Ransom, *Proc. Symposium on Modern Optics* (Polytechnic Institute of Brooklyn, New York, 1967).
4. M. M. Sondhi, J. Acoust. Soc. Am. **46**, 1158 (1969).
5. Y. Aoki, IEEE Trans. Audio Electroacoust. **AE-8**, 258 (1970).
6. J. W. Goodman, *Introduction to Fourier Optics* (McGraw-Hill, New York, 1968).
7. L. H. Enloe, Bell System Tech. J. **46**, 1479 (1967).
8. J. W. Cooley and J. W. Tukey, Math. Computat. **19**, 297 (1965).
9. G. Bergland, IEEE Spectrum **6**, 41 (1969).
10. E. L. O'Neill, *Introduction to Statistical Optics* (Addison-Wesley, Reading, Mass., 1963).
11. E. Lalor, J. Math. Phys. **9**, 2001 (1968).
12. L. B. Lesem, P. M. Hirsch, and J. A. Jordan, Jr., *Proc. Symposium on Modern Optics* (Polytechnic Institute of Brooklyn, New York, 1967).
13. T. S. Huang, PProc. IEEE **59**, 1335 (1972).
14. M. Born and E. Wolf, *Principles of Optics* (Pergamon, New York, 1970).